Surface modification on a porous Co-Cr scaffold fabricated by selective laser melting for bone implant applications

C.J. Han*, X. Chen†, J. W. Tan*, Y. Yao†, Q. S. Wei*, Z. Zhang†, and Y.S. Shi*

* State Key Lab of Materials Processing and Die & Mould Technology, Huazhong University of Science and Technology, Wuhan 430074, China
† Department of Stomatology, Union Hospital, Tongji Medical College, Huazhong University of Science and Technology, Wuhan 430074, China

REVIEWED

Abstract

Cobalt–chromium–molybdenum alloys with porous structures can be fabricated by additive manufacturing technique, which are attractive for use as scaffolds for bone implant applications. However, metallic implant are difficult to bond directly to living bone due to limited implant interface problems. Therefore, surface modification with scaffold material is required to improve bio-compatibility and the interface surface. In this study, a porous Co-Cr scaffold fabricated by selective laser melting was modified by electrodeposition with biocompatible silk fibroin. The surface characteristics of porous scaffold before and after surface modification were evaluated with the atomic force microscopy, scanning electron microscopy, X-ray diffraction, water contact angle measurement. The mechanical properties including elastic modulus and compressive strength, were determined by compression tests.

Introduction

Cobalt–chromium–molybdenum (CoCrMo) alloys are widely used in the development of hip and knee orthopedic prostheses, due to the excellent corrosion properties and lower cost [1]. Porous metal scaffolds are suitable to the load-bearing reparation due to high mechanical strength [2]. Porous scaffolds based upon the unit cell approach can effectively reduce their stiffness [3], leading to the reduction of stress shielding and improvement of implant longevity [4]. This necessitates the exploration of advanced manufacturing technologies, since conventional manufacturing process fail to produce the desired porosity in porous scaffolds. Advanced manufacturing processed based on layered manufacturing principles do provide an alternative for the fabrication of specific porous bone implants [5].

Selective laser melting (SLM) is an additive manufacturing (AM) technique based on a layer-by-layer manner, which can fabricate complex 3D metal products with nearly full densification directly from CAD data [6]. With high density, good mechanical properties and high dimensional accuracy [7-9], SLM is not only used to produce solid metal components as usual, but also suited to manufacture intricate porous geometries with specific shape and controllable size [10]. SLM is now considered a promising fabrication technique to be applied to orthopedic implants under load-bearing conditions [11].

Currently, studies have been focused on the manufacturing process, microstructure and mechanical properties of porous Co-Cr scaffolds, whereas didn't concern to the implantation into human body. Hazlehurst et al. evaluated the stiffness characteristics with varied porosities of square pore CoCrMo structures manufactured by SLM [12], and further illustrated the repeated manufacturability of functionally graded cellular structure in terms of strut size [13]. With regard to bone implant characteristics, more efforts should be made in terms of implant interface. Since the surface properties are essential for the metal implants to integrate well with the adjacent bone, metallic implant materials are difficult to bond directly to living bone due to their limited surface condition [14]. Therefore, surface modification with scaffold material is typically required, which can further improve bio-compatibility and the interface with biological cells [15], Silk fibroin (SF), a fibrous protein extracted from natural silk, is currently applied as a significant protein biomaterial of broad biomedical applicability [16]. The SF has been used for cell culture and tissue engineering with excellent mechanical properties, slow degradation profile, aqueous solubility and manufacturability under mild conditions in previous

literatures [17]. Recently, electrophoretic deposition (EPD) has been applied to modified the surface with SF [18], due to the short processing time, simple producing apparatus and easy control of the morphology of a deposited s [19, 20].

In the present study, we fabricated a porous Co-Cr scaffold using SLM technique and modify the surfaces with SF by EPD. The surface characteristics, pore structure and compression properties were studied using atomic force microscopy (AFM), scanning electron microscopy (SEM), thermogravimetric (TG), Fourier transform infrared spectroscopy (FTIR), X-ray diffraction (XRD) and compression tests.

Materials and methods

Materials

The porous scaffolds were built with a commercial Co-28Cr-6Mo gas-atomized spherical powder (Tiger International BioMetals Co., Ltd, China). Fig. 1a shows the SEM image of the as-received powder with a nearly spherical shape. The particle size distribution is between 1 μm and 28 μm (Fig. 1b). The chemical compositions of the Co-Cr-Mo alloy include 29.6 wt% Cr, 6.6 wt% Mo, 0.82 wt% Si and 0.3 wt% C as shown in Fig. 1c.

Silk fibroin aqueous solutions were prepared according to previous publication. Bombyx mori cocoons were boiled for 20 min in an aqueous solution of 0.02 M sodium carbonate and then rinsed thoroughly with Milli-Q water. After drying the extracted silk fibroin was then dissolved in 9.3 M lithium bromide solution at 60℃ for 4 h. Then, the solution was dialyzed against Milli-Q water using a cellulose dialysis membrane (MW = 3500, Biosharp, USA) at 4℃ for 3 days. Insoluble portions were removed by centrifugation at 1500 rpm for 30 min at 4℃. The final concentration of silk fibroin aqueous solution was about 40 mg mL^{-1} which was determined by weighing the remaining solid after drying.

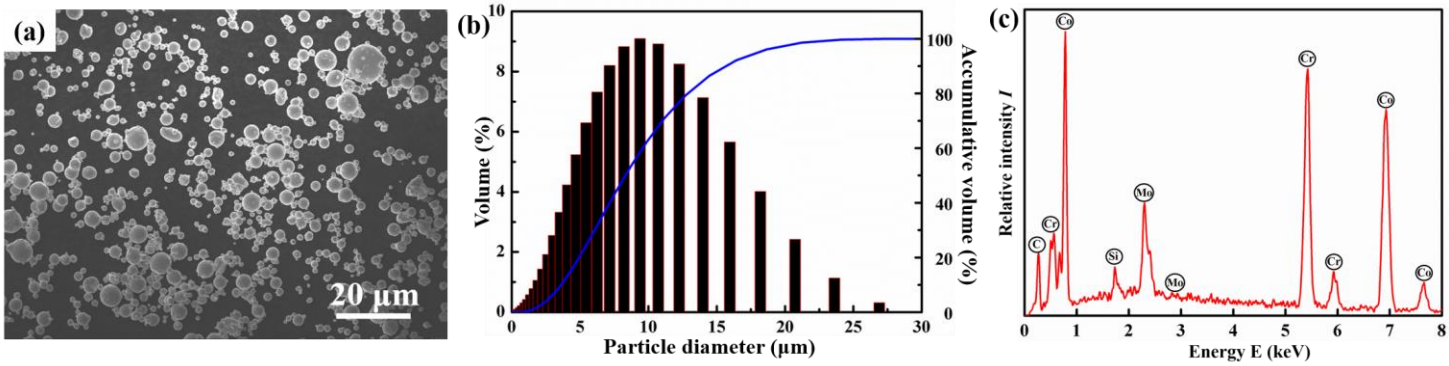

Fig. 1. (a) SEM image of the Co-Cr-Mo alloy powder; (b) particle size distribution and (c) relative contents of elements.

Manufacture and surface modification of porous Co-Cr scaffolds

Throughout this study the body-centred cubic (BCC) unit cell and its formed porous scaffolds were designed using Unigraphics NX8.0 software as shown in Fig. 2. The BCC cell is referred to as octahedral or alternatively either [±45°], containing a node located at the centre of a cube, from which all the struts radiate out to the corners of the cube [27]. The periodic porous scaffold was generated by repeating the BCC cell size of 1.25 mm. The strut size of 200 μm was designed in the BCC cell.

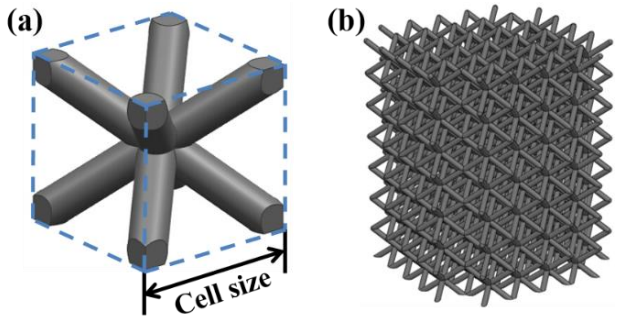

Fig. 2. CAD models of the (a) BCC unit cell and (b) generated periodic porous scaffold.

The HRPM - II SLM machine that developed by Rapid Manufacturing Center in Huazhong University of Science and Technology was adopted to manufacture the porous Co-Cr scaffolds of the BCC unit cell. The machine uses a fiber laser (redPOWER R4, SPI Lasers, UK) with the maximum power of 400 W. The processing was performed in an atmosphere filled with high purity argon in the building chamber. The BCC scaffolds were fabricated with height of 10 mm and diameter of 8 mm. All samples were manufactured using laser power of 220 W, scan line spacing of 0.07 mm, scanning speed of 300 mm/s and layer thickness of 20 μm.

The specimans were ultrasonically cleaned with acetone, ethanol, and Milli-Q water for 20 min each procedure and then rinsed with Milli-Q water. The scaffold was used as anode for EPD and parallel platinum plate as counter-electrode. The distance between the cathode and the anode was 80 mm. Deposition was performed by connecting both the cathode and the anode to a direct current power supply (Model 6614C, Agilent Technologies) with a constant voltage of 15 V for 1 min. After deposition, the electrodes were disconnected from the power supply, removed from the solution, rinsed with Milli-Q water, and finally air dried overnight.

Measurements and characterizations

The morphology of the silk fibroin was presented by atomic force microscopy (AFM, SPM9700, Japan), while the component was determined by X-ray diffraction (XRD-7000S, Japan), Fourier transform infrared spectroscopy (ATR-FTIR; Thermo Nicollet 5700, USA) and thermogravimetric (TG) analysis which was carried out on a TG/DTA thermal analyzer (STA449F3, Germany) in nitrogen atmosphere with 10℃ min^{-1} heating rate in the 40-600℃ temperature range. A JEOL-7600f Scanning Electron Microscope (JEOL, Japan) was used to study the micro structural surface characteristics and pore morphology within the scaffold, and water contact angle measurements were carried out by the sessile drop method (EasyDrop standard, KRUSS) at room temperature. Furthermore, three dimensional morphology of the porous scaffolds with or without SF was using the AFM (SPM9700, Japan), and then analysis over an area of 1 × 1 μm^2 was used to obtain average surface roughness.

Compression tests

Axial compression testing was done using an AG-IC100KN Electronic Universal Testing Machine (SHIMADZU, Japan). For all compression tests, a constant loading rate of 0.5 mm/min was used. All samples were loaded to failure along the axial direction. The maximum load of the machine was 100 KN. The stress strain data for each tested scaffold was calculated from the compressive load versus displacement data obtained from the testing with the measured dimension and gauge length, then the elastic modulus and the compressive strength were determined from stress strain curves. Three samples for Co-Cr scaffolds with or without SF were tested to determine a mean value and standard deviation for the elastic modulus and compressive strength. The microstructure morphologies of the scaffolds' fracture were observed using a JEOL-7600f Scanning Electron Microscope (JEOL, Japan).

Results and discussion

Compositions of prepared silk fibroin

Fig. 3a shows AFM images of the thin silk fibroin after natural drying treatment on the mica plate. The silk fibroin on the plate presents a smooth surface over an area of 2 × 2 μm^2. As shown from the cross-section in Fig. 3b, the starting surface contain irregular particles in the size of no more than 200 nm.

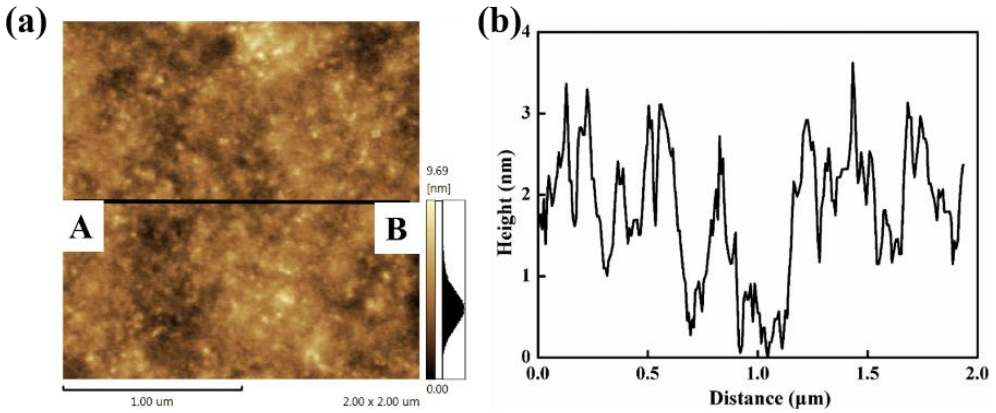

Fig. 3. (a) AFM morphology of the SF solute and (b) height value distribution along AB line.

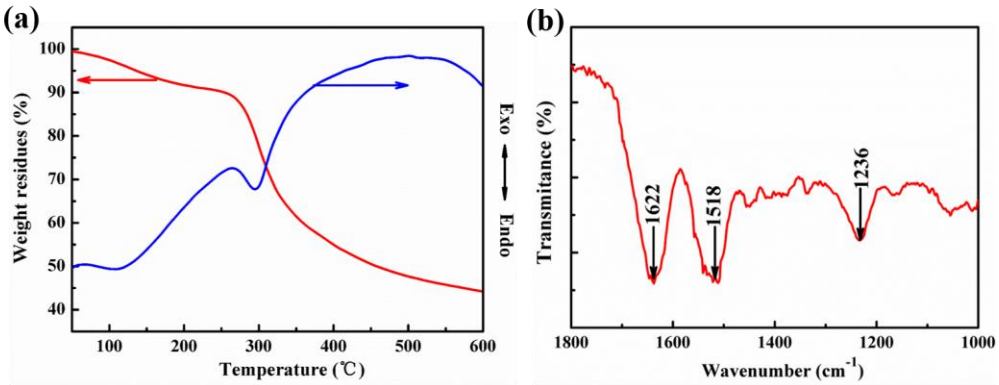

Fig. 4. Composition characterization of (a) TG and DTA curves of silk fibroin and (b) ATR-FTIR spectra of Co-Cr scaffold modified with SF.

The TG/DTA curves of silk fibroin as shown in Fig. 4a. Silk fibroin had a weight loss of 56% when the temperature was raised from 50℃ to 600℃. A notable weight loss was below 115℃， which is ascribed to the evaporation of water. The weight residue started to decline sharply at 291℃, similar to the silk fibroin with a typical decline at 285℃ [21]. As shown in Fig. 4b, the spectrum of porous Co-Cr scaffold with surface modification exhibited the characteristic bands of protein including the amide I at 1622 cm^{-1}, amide II band at 1518 cm^{-1}, and amide III band at 1236 cm^{-1}, which are the characteristic for silk fibroin [22].

Surface characteristics of modified porous scaffolds

The SEM images of porous Co-Cr scaffolds with or without surface modification in the transversal direction was shown in Fig. 5. It is obvious that some particles were bonded on the surface of struts (Fig. 5a), which may attributed to the partially melted or unmelted powder during SLM process, resulting in a rough strut surface. However, the surface quality was improved when modified with SF as shown in Fig. 5b. From the figure it can be proved that the SF was successfully covered on the struts.

The X-ray diffraction was conducted using the transverse cross section perpendicular to the building direction (Fig. 5c). The peaks from the γ phase were dominantly detected. The highest intensity is observed from (2 2 0) at 74.8 °in the Co-Cr powder, Co-Cr scaffold with or without deposited SF coating. Moreover, the intensities from (1 1 1) at 43.6 °and (2 0 0) at 50.9 °were also observed in the previous work [23, 24]. The XRD profiles reveal that no phase transformation and composition variety appear in the Co-Cr scaffold fabricated by SLM and modification with SF by EPD process.

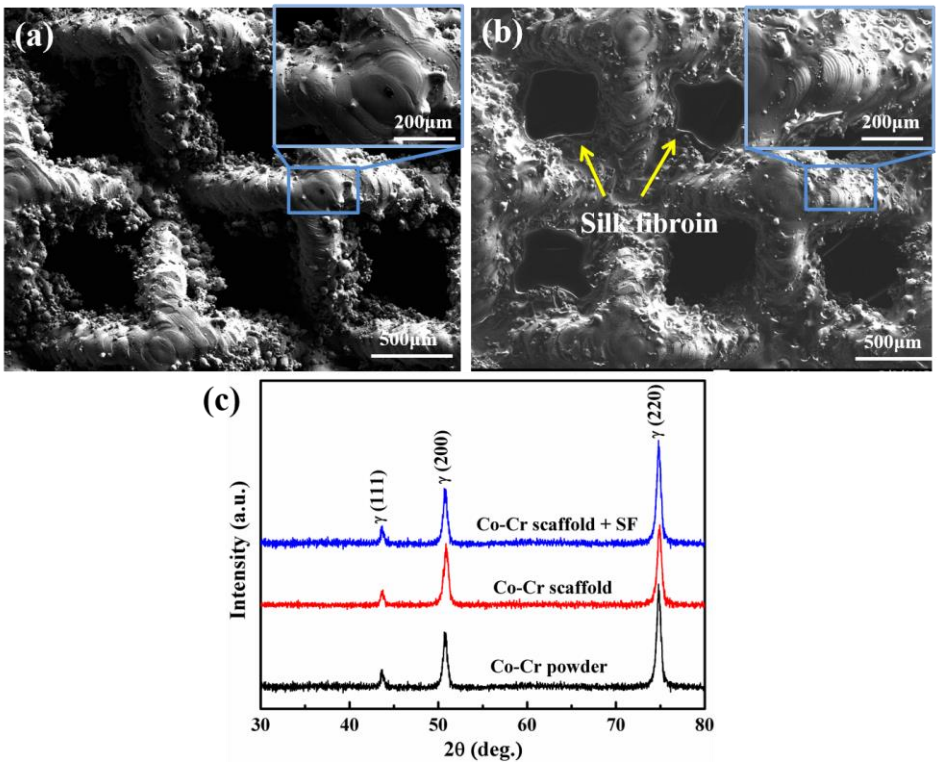

Fig. 5. SEM images of (a) porous Co-Cr scaffold, (b) scaffold modified with SF in the transversal direction and (c) XRD patterns of as-received Co-Cr powders, Co-Cr scaffolds with or without SF.

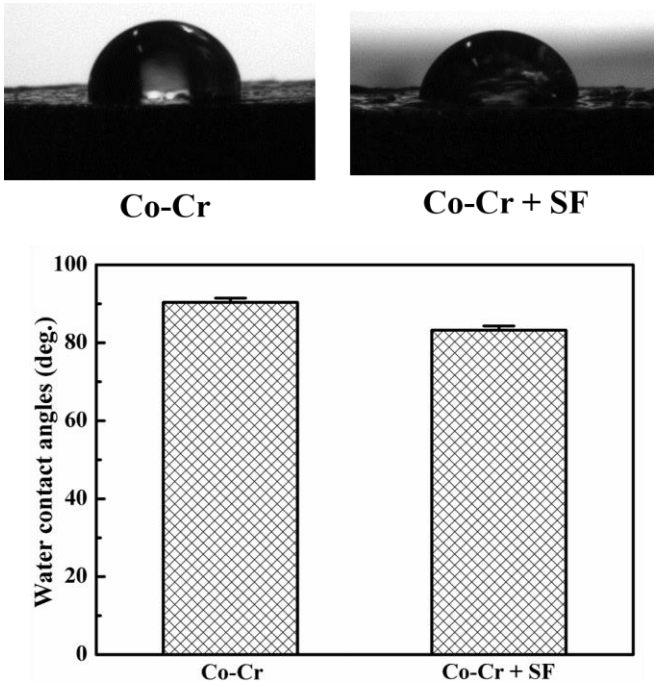

Fig. 6. Water contact angles on samples.

Surface wettability is believed to be an important factor in cells/biomaterials interactions as it may influence the cell behavior by affecting protein adsorption. To clarify the modification on the surface properties of porous Co-Cr scaffolds, water surface contact angles were measured and shown in Fig. 6. The flat Co-Cr surface has a water contact angle of 90.3 °. The Co-Cr modified with SF shows an enhanced hydrophilicity relative to Co-Cr with a water contact angle of 83.2 °. This change in the water contact angles stems from the surface chemistry. In general, efforts have been made to obtain a cell-repelling surface by making the materials surface hydrophobic because it can reduce protein adsorption. However, hydrophilic surfaces displayed better

affinity for cells. As a result, hydrophilic/hydrophobic balance of the substance surface is important for the protein absorption and the further cell attachment activity.

Fig. 7 shows the AFM analysis of the porous Co-Cr scaffolds with or without surface modification. From the topographic images, it is obvious that after modification, the as-SLMed porous scaffold presented a rough morphology (Fig. 7b) with a higher heterogeneity due to a multimodal shape on the roughness curves. As shown from the cross-sections in Fig. 7e, the coated surface contained a small grain in the size of 800 nm, while the Co-Cr sample exhibited much larger size, about 100-300 nm in diameter. After modification, the roughness curve had a more Gaussian-like shape (Fig. 7f). In Fig. 7g, the average surface roughness (Sa) measured by AFM was 1.79 ± 0.11 nm, while the Sa value was 38.11 ± 19.41 nm for the porous Co-Cr scaffolds before modification. The result indicates that the modified SF decreases the surface roughness of the as-SLMed sample. Note that surface roughness and composition are the factors that influence bone tissue reconstruction, the porous Co-Cr scaffolds modified with SF made it possible to obtain a relative smooth surface, as determined by AFM analysis. Further, the spreading of cells on the Co-Cr scaffolds with or without SF will be effected.

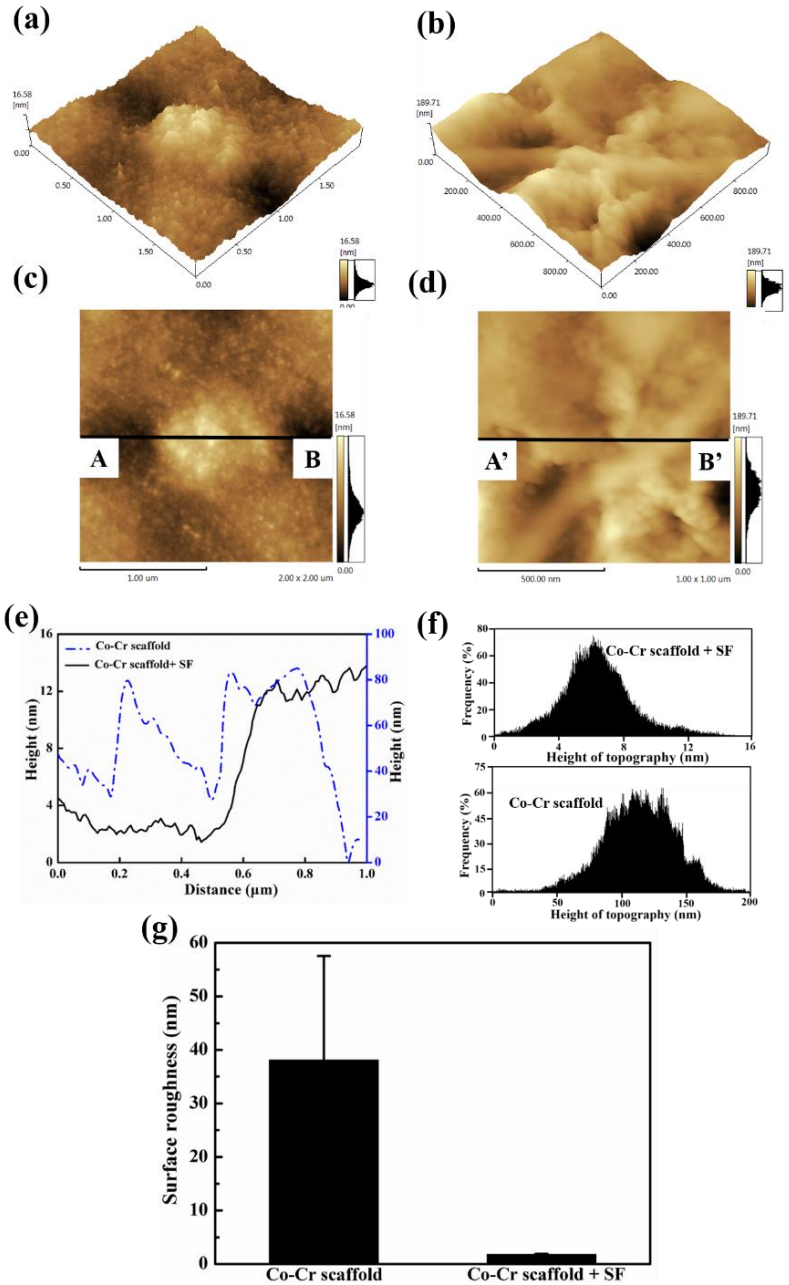

Fig. 7. AFM study of the porous Co-Cr scaffolds modified (a, c) with SF and (b, d) without SF and (e) cross section taken along the lines A-B and A'-B' located in (c) and (d) respectively and (f) surface roughness curves and (g) average values.

Mechanical properties of Co-Cr scaffold before or after surface modification

Studies have reported that surface modification on metal porous scaffolds can provide excellent mechanical properties for bone implant applications [14]. In this case, the SF was modified on the entire surface of the porous Co-Cr scaffolds in the previous sections.

Fig.8 presents the shear and tensile bond strengths of modified SF on the Co-Cr substrate. The tests rely on the bonding gel to remove the SF from the Co-Cr substrate by applying strength. The SF was detached from the Co-Cr substrate, indicating that the failures occurred at the SF-Co-Cr adhesive interface rather than SF-gel interface. The mean tensile and shear bond strengths are 2.92 ± 0.41 MPa and 3.61 ± 0.56 MPa, respectively. Therefore, failure appears easier along the longitudinal direction than that in the transversal direction.

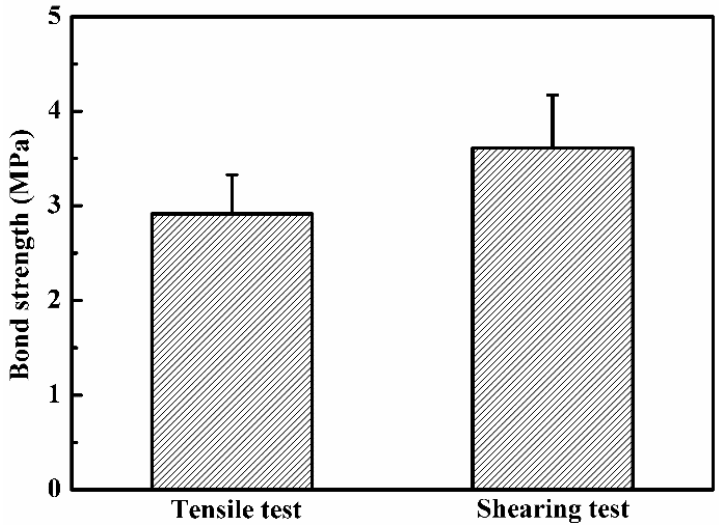

Fig. 8. Bar graph of the shear and tensile bond strengths of SF on Co-Cr substrate.

Table 1 Compression properties of Co-Cr scaffolds before and after surface modification.

Sample	Elastic modulus (GPa)	Compressive strength (MPa)
Co-Cr scaffold	2.30±0.09	76.09±1.07
Co-Cr scaffold + SF	2.53±0.05	75.71±1.66

Average elastic modulus and compressive strength of tested scaffolds as calculated are given in Table 1. The compressive elastic modulus and strength of cancellous bone in the femoral head have been stated as 2.73 GPa and 18 MPa respectively [25]. The scaffold with 1250 μm cell size obtains modulus which is similar to this type of femoral bone, but even much higher compressive strength. Note that the strengths of porous Co-Cr scaffold exhibit no significant change after EPD. However, the elastic modulus value of scaffold modified with SF is 10% higher than Co-Cr scaffold without modification. This phenomenon can be attributed to the cationization on the metal surface. Being a chemical treatment, it causes the increase of positively charged superficial groups on a protein due to the electrodeposition of SF at positive electrode [22]. In addition, because of the negative surface charge, the SF was deposited on positive electrode by EPD, resulting in the corrosion of the substrate [26]. This chemical corrosion treatment will enhance the mechanical properties of scaffolds. In fact, it shows that compression properties of coated scaffolds exhibit no worse than those without surface modification. Future work will be focused on the cell culture of porous Co-Cr scaffolds before and after surface modification.

Conclusions

This study prepared a porous Co-Cr scaffold with surface modification using SLM and EPD process. The FTIR spectrum and SEM images of microstructure show that the silk fibroin can be deposited on the surface of porous Co-Cr scaffold, improving the surface quality of as-SLMed struts. The Co-Cr modified with

SF shows an enhanced hydrophilicity by water contact angle tests, which displayed better affinity for cells. Through AFM analysis, the porous Co-Cr scaffold surface treated with SF exhibits a smooth nanostructured surface with average surface roughness of 1.79 nm that can effectively induce cell spreading.

The mean tensile and shear bond strengths of SF coating are 2.92 MPa and 3.61 MPa respectively, illustrating that failure appears easier along the longitudinal direction than that in the transversal direction. Compared with the strength of 76.1 MPa and modulus of 2.3 GPa, the porous scaffold exhibits a high mechanical strength of 75.7 MPa and an elastic modulus of 2.5 GPa after surface modification, resembling the modulus of cancellous bone. It shows that compression properties of modified scaffolds exhibit no worse than those without surface modification.

Acknowledgement

The work described in this paper were supported by the funding sources from The State Key Laboratory of Material Processing and Die & Mould Technology in Huazhong University of Science and Technology, China (Grant Nos. 2012-P02 and 2013-09), National Key Technology R&D Program of Ministry of Science and Technology of China (Grant No. 2012BAF08B03), and National Natural Science Foundation of China (Grant No. 51375188 and 51375189).

Reference

[1] Williams DF. On the mechanisms of biocompatibility. Biomaterials 2008; 29:2941-53.
[2] Ryan G, Pandit A, Apatsidis DP. Fabrication methods of porous metals for use in orthopaedic applications. Biomaterials 2006; 27:2651-70.
[3] Yan C, Hao L, Hussein A, Raymont D. Evaluations of cellular lattice structures manufactured using selective laser melting. International Journal of Machine Tools and Manufacture 2012; 62:32-8.
[4] Gong H, Wu W, Fang J, Dong X, Zhao M, Guo T. Effects of materials of cementless femoral stem on the functional adaptation of bone. Journal of Bionic Engineering 2012; 9:66-74.
[5] Parthasarathy J, Starly B, Raman S, Christensen A. Mechanical evaluation of porous titanium (Ti6Al4V) structures with electron beam melting (EBM). Journal of the mechanical behavior of biomedical materials 2010; 3:249-59.
[6] Kruth J-P, Vandenbroucke B, Vaerenbergh vJ, Mercelis P. Benchmarking of different SLS/SLM processes as rapid manufacturing techniques. 2005.
[7] Brandl E, Heckenberger U, Holzinger V, Buchbinder D. Additive manufactured AlSi10Mg samples usingSelective Laser Melting (SLM): Microstructure, high cycle fatigue, and fracture behavior. Materials & Design 2012; 34:159-69.
[8] Warnke PH, Douglas T, Wollny P, Sherry E, Steiner M, Galonska S, et al. Rapid prototyping: porous titanium alloy scaffolds produced by selective laser melting for bone tissue engineering. Tissue engineering part c: Methods 2008; 15:115-24.
[9] Amato KN, Gaytan SM, Murr LE, Martinez E, Shindo PW, Hernandez J, et al. Microstructures and mechanical behavior of Inconel 718 fabricated by selective laser melting. Acta Materialia 2012; 60:2229-39.
[10] Mullen L, Stamp RC, Brooks WK, Jones E, Sutcliffe CJ. Selective Laser Melting: A regular unit cell approach for the manufacture of porous, titanium, bone in‐growth constructs, suitable for orthopedic applications. Journal of Biomedical Materials Research Part B: Applied Biomaterials 2009 ;89:325-34.
[11] Ahmadi S, Campoli G, Yavari SA, Sajadi B, Wauthlé R, Schrooten J, et al. Mechanical behavior of regular open-cell porous biomaterials made of diamond lattice unit cells. Journal of the mechanical behavior of biomedical materials 2014; 34:106-15.
[12] Hazlehurst K, Wang CJ, Stanford M. Evaluation of the stiffness characteristics of square pore CoCrMo cellular structures manufactured using laser melting technology for potential orthopaedic applications. Materials & Design 2013; 51:949-55.

[13] Hazlehurst KB, Wang CJ, Stanford M. An investigation into the flexural characteristics of functionally graded cobalt chrome femoral stems manufactured using selective laser melting. Materials & Design 2014; 60:177-83.
[14] Wang X, Li Y, Hodgson PD, Wen Ce. Biomimetic modification of porous TiNbZr alloy scaffold for bone tissue engineering. Tissue Engineering Part A 2009; 16:309-16.
[15] Dumée LF, He L, Lin B, Ailloux F-M, Lemoine J-B, Velleman L, et al. The fabrication and surface functionalization of porous metal frameworks–a review. Journal of Materials Chemistry A 2013; 1:15185-206.
[16] Lu Q, Wang X, Hu X, Cebe P, Omenetto F, Kaplan DL. Stabilization and release of enzymes from silk films. Macromolecular bioscience 2010; 10:359-68.
[17] Wenk E, Merkle HP, Meinel L. Silk fibroin as a vehicle for drug delivery applications. Journal of Controlled Release 2011; 150:128-41.
[18] Zhang Z, Jiang T, Ma K, Cai X, Zhou Y, Wang Y. Low temperature electrophoretic deposition of porous chitosan/silk fibroin composite coating for titanium biofunctionalization. Journal of Materials Chemistry 2011; 21:7705-13.
[19] Mehdipour M, Afshar A, Mohebali M. Electrophoretic deposition of bioactive glass coating on 316L stainless steel and electrochemical behavior study. Applied Surface Science 2012; 258:9832-9.
[20] Li M, Liu Q, Jia Z, Xu X, Shi Y, Cheng Y, et al. Electrophoretic deposition and electrochemical behavior of novel graphene oxide-hyaluronic acid-hydroxyapatite nanocomposite coatings. Applied Surface Science 2013; 284:804-10.
[21] Tsukada M, Obo M, Kato H, Freddi G, Zanetti F. Structure and dyeability of Bombyx mori silk fibers with different filament sizes. Journal of applied polymer science 1996; 60:1619-27.
[22] Zhang Z, Qu YY, Li XS, Zhang S, Wei QS, Shi YS, et al. Electrophoretic deposition of tetracycline modified silk fibroin coatings for functionlization of titanium surfaces. Applied Surface Science 2014; 303:255-62.
[23] Sato Y, Nomura N, Fujinuma S, Chiba A. Fabrication of gas atomized Co-Cr-Mo alloy powder and microstructure of the hot-pressed compacts. Journal of the Japan Institute of Metals 2006; 70:275-80.
[24] Takaichi A, Suyalatu, Nakamoto T, Joko N, Nomura N, Tsutsumi Y, et al. Microstructures and mechanical properties of Co-29Cr-6Mo alloy fabricated by selective laser melting process for dental applications. J Mech Behav Biomed Mater 2013; 21:67-76.
[25] Öhman C, Baleani M, Perilli E, Dall'Ara E, Tassani S, Baruffaldi F, et al. Mechanical testing of cancellous bone from the femoral head: experimental errors due to off-axis measurements. Journal of biomechanics 2007; 40:2426-33.
[26] Lundgren M, Allan NL, Cosgrove T. Modeling of wetting: a study of nanowetting at rough and heterogeneous surfaces. Langmuir 2007; 23:1187-94.